

https://dspace.org/

The effect of blasting on the rockmass for designing the most effective preconditioning blasts in deep-level gold mines

Toper, Ali Zafer

2011-04-18
http://hdl.handle.net/10539/9499

Downloaded from a DSpace repository. https://dspace.org/

The copyright of the above-mentioned described thesis rests with the author or the University to which it was submitted. No portion of the text derived from it may be published without the prior written consent of the author or University (as may be appropriate). *Short quotations may be included in the text of a thesis* or dissertation for purposes of illustration, comment or criticism, provided full acknowledgement is made of the source, author and University.

UNIVERSITY OF THE WITWATERSRAND

Ph.D. Thesis

THE EFFECT OF BLASTING ON THE ROCKMASS FOR DESIGNING THE MOST EFFECTIVE PRECONDITIONING BLASTS IN DEEP-LEVEL GOLD MINES

Ali Zafer Toper

A thesis submitted to the Faculty of Engineering, University of the Witwatersrand, Johannesburg, in fulfilment of the requirements for the degree of Doctor of Philosophy.

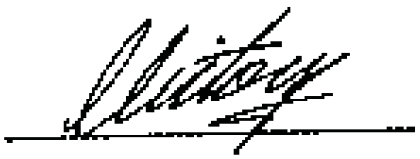
Johannesburg, June 2003

DECLARATION

I declare that this thesis is produced mainly from the results obtained from a research project funded by Safety in Mines Research Advisory Committee (SIMRAC) and that some parts of it (e.g. measurements, analysis, interpretations, etc.) were provided by other members of the research team of CSIR Division of Mining Technology (see Acknowledgements section).

It is being submitted for the Degree of Doctor of Philosophy in the University of the Witwatersrand, Johannesburg.

This thesis has not been submitted before for any degree or examination in any other University but some parts of it were published in some local and international journals and presented at various seminars and conferences.



Ali Zafer Toper

23rd. day of JUNE (year) 2003

ABSTRACT

According to the accident database compiled by CSIR Division of Mining Technology (Miningtek), a significant percentage of fatalities have resulted from faceburst incidents throughout the South African gold mining industry. In order to address this problem, an extensive research programme has been undertaken.

Two different preconditioning techniques have been developed; namely, face-perpendicular preconditioning and face-parallel preconditioning. Both have prevented face bursting in the areas to which they have been applied, even though several large seismic events have occurred close to the faces in some areas. In addition, minimal overall damage was observed in the preconditioned panels following these events, compared to similarly exposed unpreconditioned panels. Preconditioning has also provided some protection from distant events to the face area, through the capacity of the preconditioned ground to absorb energy.

Although the main purpose of preconditioning was to prevent facebursts, an improvement in hangingwall stability and a significant increase in the face advance rate, consistent with improved fragmentation, have been noted in preconditioned areas. During preconditioning, the average face advance rate increased significantly compared with unpreconditioned periods. Owing to this increase in face advance rate, the mining cost per area mined decreased in preconditioned panels. The effect of preconditioning on improving the drilling rate of production holes was also significant. The preconditioning experiments also indicated that it was possible to implement this method in a deep-level longwall mining environment without significant disruption to the mining cycle. Guidelines for both preconditioning techniques have been compiled.

In order to determine the optimum blast parameters for achieving the most effective preconditioning, an extensive optimisation study was carried out for the face-perpendicular preconditioning technique. While optimum values for parameters such as hole length, diameter and spacing were determined, it was ultimately concluded that the differences in results obtained by varying the

preconditioning parameters were less significant than the clear positive differences observed when comparing preconditioned areas with non-preconditioned areas.

In order to assure successful implementation of the techniques in the mining environment, a structured implementation procedure has been developed from experience gained at research sites. This procedure consists of education and training of all levels of the production personnel as well as the personnel of the training and safety departments of the mine.

In memory of all mine workers

who lost their life

as a result of

rockburst accidents

ACKNOWLEDGEMENTS

I would like to gratefully acknowledge that the work reported in this thesis was made possible by funding provided by Safety in Mines Research Advisory Committee (SIMRAC) and forms part of the rockburst control research programme carried out by the CSIR / Miningtek.

I wish to acknowledge the contribution of other members of the project team, namely: N. Lightfoot, *D. H. Kullmann, R. D. Stewart, M. Grodner, A. L. Janse van* Rensburg and the late P. J. Longmore of CSIR / Miningtek, D. J. Adams of SIMPROSS, and P. Brenchley of Anglogold, who provided me with the results of monitoring and measurements, *data analysis, and invaluable insights used in this* thesis. I would like to thank N. Lightfoot and D. H. Kullmann, for providing me with their contribution on the mechanism of preconditioning and the results obtained from face-parallel preconditioning experiments; *R. D. Stewart, for all seismic data* analysis; and M. Grodner, for all fracture mapping and hangingwall profiling studies.

The work has enjoyed the cooperation and support of the South African gold mining industry, and in particular that of Driefontein Consolidated, Mponeng (ex-Western Deep Levels South Mine) and Blyvooruitzicht gold mines where the main research sites were situated. I would like to thank the management of all three mines for their cooperation in allowing the field sites to operate on their mines. In addition, I would like to express my gratitude to the rock engineering departments and production personnel on these mines who gave vaulable assistance during the course of the field experiments. Without the help of the people on the mines none of this work would have been possible.

I would like to thank Dr. J. A. L. Napier and Dr. M. K. C. Roberts of CSIR / Miningtek and Prof. T. R. Stacey of the University of Witwatersrand for reviewing this thesis and providing me with several useful comments and many helpful suggestions.

I also would like to thank Prof. R. G. Gürtunca and Dr. D. F. Malan of CSIR / Miningtek for encouraging me to finish this thesis.

Finally, I would like to thank my wife Şengül and my daughter Ezgi for their enthusiastic support and understanding during the writing of this thesis.

CONTENTS

		Page
DECLARATION		2
ABSTRACT		3
ACKNOWLEDGEMENTS		6
CONTENTS		8
LIST OF FIGURES		13
LIST OF TABLES		23
1	**INTRODUCTION**	**25**
1.1	Research problem	25
1.2	Rockburst control research programme	26
1.3	Objectives of this study	28
1.4	Outline of the content of the thesis	29
2	**LITERATURE REVIEW**	**31**
2.1	Introduction	31
2.2	Historical development	31
2.3	Early research initiatives	34
2.4	Rockbursts	38
2.4.1	Description and types of rockbursts	38
2.4.2	Control of rockbursts	42
2.5	Destressing / preconditioning	45
2.5.1	The principle and objectives	48
2.5.2	Field Trials	51
2.6	Summary	64

3	**THE EFFECTS OF PRECONDITIONING BLASTS IN CONFINED ROCK**	**65**
3.1	Introduction	65
3.2	Objectives	66
3.3	Test programme	66
3.3.1	Test site	67
3.3.2	Instrumentation and monitoring	68
3.4	Blast monitoring	69
3.4.1	Introduction	69
3.4.2	Instrumentation	70
3.4.3	Results of blast monitoring	73
3.5	Ground Penetrating Radar (GPR) investigations	80
3.6	Production blasts and fracture mapping	81
3.7	Studies on rock samples	85
3.7.1	Rock Quality Designation (RQD)	85
3.7.2	Rock testing	87
3.8	Stress determination studies	87
3.9	Numerical modelling	99
3.10	Summary	114
4	**FACE-PARALLEL PRECONDITIONING**	**116**
4.1	Introduction	116
4.2	Summary of findings from test site	117
4.2.1	Site description	117
4.2.2	Preconditioning layout	117
4.2.3	Instrumentation and monitoring programme	119
4.2.4	Summary of preconditioning activity	122
4.2.5	Analysis of preconditioning blasts	122
4.2.6	Quantitative analysis of the effects of preconditioning	124
4.3	Guidelines for face-parallel preconditioning	151
4.3.1	Introduction	151
4.3.2	Drilling of preconditioning holes	151

4.3.3 Charging of preconditioning holes 154
4.3.4 Stemming 155
4.3.5 Dealing with misfires 157
4.3.6 Assessing the effectiveness of preconditioning blasts 158
4.3.7 Blast optimisation 158
4.4 Summary 159

5 FACE-PERPENDICULAR PRECONDITIONING 161

5.1 Introduction 161
5.2 Test site 161
5.2.1 Preconditioning layout 163
5.2.2 Instrumentation and monitoring programme 168
5.3 Qualitative analysis of the effects of preconditioning 174
5.3.1 Ground conditions 174
5.3.2 Rockburst damage 176
5.3.3 Workers' perceptions 179
5.4 Quantitative analysis of the effects of preconditioning 181
5.4.1 Seismic activity 182
5.4.2 Convergence measurements 187
5.4.3 Fracturing in the stope hangingwall 193
5.4.4 Hangingwall profiles 203
5.4.5 Stress determination 204
5.4.6 Fragmentation 207
5.4.7 Ground Penetrating Radar 209
5.4.8 Safety records 210
5.4.9 Production 212
5.4.10 Cost analysis 214
5.5 Optimisation of the technique 218
5.5.1 Seismic activity 218
5.5.2 Rockmass fracturing 227
5.5.3 Hangingwall profiles 230
5.5.4 Ground Penetrating Radar surveys 230

5.5.5 Convergence measurements 234
5.5.6 *Production* 235
5.6 Preconditioning in high-stoping-width areas 238
5.6.1 Summary of findings 239
5.7 Guidelines for face-perpendicular preconditioning 246
5.7.1 Introduction 246
5.7.2 Drilling of preconditioning holes 247
5.7.3 Charging of preconditioning holes 251
5.7.4 Stemming 252
5.7.5 *Handling of misfires and sockets* 254
5.8 Summary 254

6 THE MECHANISM OF PRECONDITIONING 256

6.1 Introduction 256
6.2 *Preconditioning mechanism* 257
6.2.1 Numerical modelling of the mechanics of preconditioning 257
6.2.2 Influence of stress waves and gas pressurisation 262
6.2.3 Rockmass response to preconditioning 267
6.2.4 The effect of preconditioning on stress-wave transmission through discontinuous rock 272
6.2.5 Postulated preconditioning mechanism 273
6.3 Summary 277

7 IMPLEMENTATION OF PRECONDITIONING 279

7.1 Introduction 279
7.2 Implementation experiments 280
7.3 Key issues in implementation 290
7.4 A structured implementation procedure 298
7.4.1 Preliminary evaluation 298
7.4.2 Planning of the implementation programme 298
7.4.3 *Education and training* seminars and workshops 299
7.4.4 Risk assessment 301

7.4.5 On-the-job training 301
7.4.6 Follow-up and assessment of the results 302
7.5 Summary 303

8 DISCUSSION AND CONCLUSIONS 304

8.1 Effects of preconditioning blasts in confined rock 304
8.2 Preconditioning techniques 305
8.3 Preconditioning mechanism 307
8.4 Safety and productivity 310
8.5 Optimisation of preconditioning 311
8.6 Implementation of preconditioning 313
8.7 Assessment of the effects of preconditioning 314

9 RECOMMENDED FUTURE RESEARCH 317

APPENDIX A: CRITERIA BY WHICH PRECONDITIONING BLASTS WERE JUDGED 318

APPENDIX B: SUMMARY INFORMATION FOR EACH PRECONDITIONING BLAST 321

APPENDIX C: EDUCATION AND TRAINING MODULE 326

APPENDIX D: AN EXAMPLE OF RISK ASSESSMENT ON PRECONDITIONING 336

REFERENCES 343

LIST OF FIGURES

Figure		Page
Figure 3.4.1	Scaled section of the blastholes from each test	70
Figure 3.4.2	Schematics of the tunnel faces, showing the relative positions of the blasthole, accelerometer and doorstopper holes	71
Figure 3.4.3	Schematic section through an instrument hole, showing the installation technique for accelerometers	72
Figure 3.4.4	Peak accelerations vs. distance from blasthole	76
Figure 3.4.5	Peak velocities vs. distance from blasthole	77
Figure 3.4.6	The detonation velocities measured during the 1st, 2nd and 3rd test blasts	80
Figure 3.6.1	Ground Penetrating Radar scans before (left) and after (right) the third test blast	82
Figure 3.6.2	Schematic view of induced fracturing by test blasts (not to scale)	84
Figure 3.7.1	Rock Quality Designation (RQD) and average core sample lengths, before (BB) and after (AB) the second test blast	86
Figure 3.7.2	Rock Quality Designation (RQD) and average core sample lengths, before (BB) and after (AB) the third test blast	86
Figure 3.8.1	Principal stresses calculated from strain gauge measurements (1.5 m away from blasthole). Test blast 1	89
Figure 3.8.2	Principal stresses calculated from strain gauge measurements (1.5 m away from blasthole). Test blast 2	89
Figure 3.8.3	Principal stresses calculated from strain gauge measurements (2 m away from blasthole). Test blast 2	89
Figure 3.8.4	Principal stresses calculated from strain gauge measurements (1 m away from blasthole). Test blast 3	90
Figure 3.8.5	Principal stresses calculated from strain gauge measurements (1.5 m away from blasthole). Test blast 3	90
Figure 3.8.6	Principal stresses calculated from strain gauge measurements (2 m away from blasthole). Test blast 3	90

Figure 3.8.7 Principal stresses calculated from strain gauge measurements at varying distances away from blasthole, Test blast 3 91
Figure 3.8.8 Principal stresses calculated from strain gauge measurements at 5 m depth (1 m away from blasthole), Test blast 4 91
Figure 3.8.9 Principal stresses calculated from strain gauge measurements at 4 m depth (1.5 m away from blasthole), Test blast 4 92
Figure 3.8.10 Principal stresses calculated from strain gauge measurements at 5 m depth (1.5 m away from blasthole), Test blast 4 92
Figure 3.8.11 Principal stresses calculated from strain gauge measurements at 6 m depth (1.5 m away from blasthole), Test blast 4 92
Figure 3.8.12 Principal stresses calculated from strain gauge measurements at 5 m depth (2 m away from blasthole), Test blast 4 93
Figure 3.8.13 Principal stresses calculated from strain gauge measurements at various distances from blasthole, Test blast 4 93
Figure 3.8.14 Principal stresses calculated from strain gauge measurements at various depths (1.5 m away from blasthole), Test blast 4 93
Figure 3.8.15 Orientation of principal stresses before and after test blasts 1 & 2 95
Figure 3.8.16 Orientation of principal stresses before and after test blast 3 96
Figure 3.8.17 Orientation of principal stresses before and after test blast 4 97
Figure 3.8.18 Orientation of principal stresses before and after test blast 4 98
Figure 3.9.1 Plot of stress vectors (Model 1: no bedding plane, blast pressure = 500 MPa) 102
Figure 3.9.2 Plot of displacement vectors (Model 1: no bedding plane, blast pressure = 500 MPa) 102
Figure 3.9.3 Plot of major principal stress contours (Model 1: no bedding plane, blast pressure = 500 MPa) 103

Figure 3.9.4 Plot of minor principal stress contours (Model 1: no bedding plane, blast pressure = 500 MPa) 103
Figure 3.9.5 Plot of stress vectors (Model 2: bedding planes: 0°, blast pressure = 500 MPa) 104
Figure 3.9.6 Plot of displacement vectors (Model 2: bedding planes: 0°, blast pressure = 500 MPa) 104
Figure 3.9.7 Plot of major principal stress contours (Model 2: bedding planes: 0°, blast pressure = 500 MPa) 105
Figure 3.9.8 Plot of minor principal stress contours (Model 2: bedding planes: 0°, blast pressure = 500 MPa) 105
Figure 3.9.9 Plot of stress vectors (Model 3: bedding planes: 30°, blast pressure = 500 MPa) 106
Figure 3.9.10 Plot of displacement vectors (Model 3: bedding planes: 30°, blast pressure = 500 MPa) 106
Figure 3.9.11 Plot of major principal stress contours (Model 3: bedding planes: 30°, blast pressure = 500 MPa) 107
Figure 3.9.12 Plot of minor principal stress contours (Model 3: bedding planes: 30°, blast pressure = 500 MPa) 107
Figure 3.9.13 Plot of stress vectors (Model 4: bedding planes: 30°, blast pressure = 1000 MPa) 109
Figure 3.9.14 Plot of displacement vectors (Model 4: bedding planes: 30°, blast pressure = 1000 MPa) 108
Figure 3.9.15 Plot of major principal stress contours (Model 4: bedding planes: 30°, blast pressure = 1000 MPa) 109
Figure 3.9.16 Plot of minor principal stress contours (Model 4: bedding planes: 30°, blast pressure = 1000 MPa) 109
Figure 3.9.17 Plot of stress vectors (Model 5: bedding planes: 60°, blast pressure = 500 MPa) 110
Figure 3.9.18 Plot of displacement vectors (Model 5: bedding planes: 60°, blast pressure = 500 MPa) 110
Figure 3.9.19 Plot of major principal stress contours (Model 5: bedding planes: 60°, blast pressure = 500 MPa) 111
Figure 3.9.20 Plot of minor principal stress contours (Model 5: bedding planes: 60°, blast pressure = 500 MPa) 111

Figure 3.9.21 Plot of stress vectors (Model 6: bedding planes: 90°, blast pressure = 500 MPa) 112
Figure 3.9.22 Plot of displacement vectors (Model 6: bedding planes: 90°, blast pressure = 500 MPa) 112
Figure 3.9.23 Plot of major principal stress contours (Model 6: bedding planes: 90°, blast pressure = 500 MPa) 113
Figure 3.9.24 Plot of major principal stress contours (Model 6: bedding planes: 90°, blast pressure = 500 MPa) 113
Figure 4.2.1 Plan of 17-24W stope (test site) and layout of the microseismic network around the mining faces 118
Figure 4.2.2 Preconditioning layout at the test site (17-24W stope) 120
Figure 4.2.3 Plan of the preconditioning test site, showing the geophone positions for the PSS network 120
Figure 4.2.4 Comparison of the recorded preconditioning blast event magnitudes with the amount of explosive used for each blast 125
Figure 4.2.5 Seismic data recorded during and following a preconditioning blast at the test site on 26 November 1992 126
Figure 4.2.6 Seismic data recorded during and following a preconditioning blast at the test site on 22 December 1993 127
Figure 4.2.7 Seismic data recorded during and following a preconditioning blast at the test site on 31 March 1993 128
Figure 4.2.8 Seismic data recorded during and following a preconditioning blast at the test site on 28 October 1994 129
Figure 4.2.9 Seismic data recorded during and following a preconditioning blast at the test site on 10 January 1995 130
Figure 4.2.10 Seismic data recorded during and following the preconditioning blasts at the test site on 11 April and 15 April 1994 132
Figure 4.2.11 The stope face appearance after a preconditioning blast 137
Figure 4.2.12 Three-dimensional surface plots of the stope face for (a) before and (b) after a preconditioning blast 138
Figure 4.2.13 A contoured plot of the difference in measurements before and after a preconditioning blast 139
Figure 4.2.14 Schematic view of fracture groups (not to scale) 140

Figure 4.2.15 (a) Sketch plan showing the orientation of the various fracture groups in relation to the 17-24W pillar, (b) Plot of seismic events (blue circles) recorded after a preconditioning blast (red star) 142
Figure 4.2.16 Plot of the straight ray apparent velocity measured between common shot and receiver hole numbers, showing the velocity variation from east to west (after Maxwell and Young, 1995) 144
Figure 4.2.17 Straight ray velocity image produced from the seismic tomography survey (after Maxwell and Young, 1995) 146
Figure 4.2.18 Plan of the locations of the larger seismic events recorded prior to seismic tomography experiment 147
Figure 4.2.19 Time section along line A–B of Figure 4.2.18 148
Figure 4.2.20 Velocity image of Figure 4.2.17 reconstructed through curved ray tracing (after Carneiro, 1995) 149
Figure 4.2.21 Straight ray tomographic image of the velocity change following the preconditioning blast (after Maxwell and Young, 1995) 150
Figure 4.2.22 Plan of the seismicity (filled circles) recorded after the preconditioning blast (filled star) 150
Figure 4.3.1 Face-parallel preconditioning layout in an overhand mining sequence (not to scale) 152
Figure 4.3.2 Effects of positioning a large (~89 mm diameter) preconditioning hole at varying distances ahead of the slope face 153
Figure 4.3.3 (a) Use of second hole, parallel to main hole, to precondition stemmed area. (b) Use of additional holes, perpendicular to panel face, to precondition stemmed area 157
Figure 5.2.1 Test site (87-49W stope), showing different phases of mining 163
Figure 5.2.2 Ground Penetrating Radar scans before and after the test blast 165
Figure 5.2.3 Layout of face-perpendicular preconditioning holes, showing radius of influence of each hole (r = 1.5 m) and the recommended spacing between holes (i.e. 3 m) 166

Figure 5.2.4	Section of stope face showing the preconditioning hole prior to blasting	167
Figure 5.2.5	Preconditioning as an integral part of ordinary fuse and igniter cord tie-up system	169
Figure 5.2.6	Plan of a portion of the Mponeng gold mine, showing the positions of the 84-49W stability pillar and of the 87-49W stope, which is the preconditioning experiment site	170
Figure 5.2.7	Plan of the preconditioning site, showing the layout of the PSS network monitoring the experiment. The triaxial geophone positions are indicated by squares labelled 'OS1i' to 'OS5i'	171
Figure 5.2.8	Plan of a portion of Mponeng gold mine, showing the updated configuration of the preconditioning site seismic network	172
Figure 5.2.9	The relative positions of all convergence stations installed at the project site	173
Figure 5.3.1	The improvement in hangingwall conditions brought about by the introduction of preconditioning	174
Figure 5.3.2	A comparison of hangingwall conditions in unpreconditioned and preconditioned portion of a panel	175
Figure 5.3.3	Improved face and hangingwall conditions in a preconditioned panel	176
Figure 5.3.4	Schematic plan of West 2 diagonal panel where a rockburst resulted in extensive damage and five injuries (not to scale)	178
Figure 5.3.5	Seismic events of M>1 recorded from the test site between 26/08/96 and 20/10/96	180
Figure 5.4.1	Plan of the seismicity recorded from the preconditioning test site during 1995 (seismic events of magnitude M ≥0 are shown)	183
Figure 5.4.2	Plan of preconditioning site, showing mining faces	185
Figure 5.4.3	Measurements from convergence station A	189
Figure 5.4.4	Measurements from convergence station B	189
Figure 5.4.5	Measurements from convergence station C	190
Figure 5.4.6	Measurements from convergence station D	190
Figure 5.4.7	Positions of convergence stations	191

Figure 5.4.8	Plot of convergence measurements, showing the effect of seismicity on total convergence rate and comparison of elastic and inelastic components of total convergence	191
Figure 5.4.9	Average convergence rates of all (51) stations at the preconditioning test site	192
Figure 5.4.10	Schematic view of fracture groups (not to scale)	194
Figure 5.4.11	Summary of orientation data of fractures mapped prior to and after the initiation of preconditioning (after Grodner, 1997)	195
Figure 5.4.12	Pie charts of orientations of fractures prior to and after preconditioning (after Grodner, 1997)	198
Figure 5.4.13	Orientation of face-parallel fractures in diagonal and up-dip panels	199
Figure 5.4.14	Graph showing relative abundance of the various fracture groups in normal and preconditioned areas	202
Figure 5.4.15	Variation in profile length and gradient between preconditioning holes	203
Figure 5.4.16	Solid inclusion cell designed to measure strain changes in fractured rock	205
Figure 5.4.17	Calibration of solid inclusion cell at the test laboratory	205
Figure 5.4.18	The measured strains of the three strain gauges in the B90 rosette (on a plane parallel to face)	206
Figure 5.4.19	Stress profile ahead of an advancing face as obtained from strain measurements taken underground	206
Figure 5.4.20	The averaged projected areas (size) of fragments from preconditioned and unpreconditioned panels	209
Figure 5.4.21	The fragment size distribution in preconditioned and unpreconditioned panels	209
Figure 5.4.22	Ground Penetrating Radar scan of an unpreconditioned panel face and a preconditioned panel face, showing the density of open fractures	211
Figure 5.4.23	Ground Penetrating Radar scan of a preconditioned panel face, showing the depth of the remobilised fracture zone	212
Figure 5.5.1	Seismic data recorded from 26/08/96 to 20/10/96 by Portable Seismic System	219

Figure 5.5.2	Plan of the test site, showing three actively mined up-dip panels	220
Figure 5.5.3	Seismic data recorded between 26/08/96 and 20/10/96 from the test site by PSS	221
Figure 5.5.4	Frequency-magnitude distribution of seismic data recorded from the test site between 26/08/96 and 20/10/96 by PSS	222
Figure 5.5.5	Cumulative number of seismic events recorded from the test by PSS	222
Figure 5.5.6	Diurnal distribution of seismic data recorded from the test stope between 26/08/96 and 20/10/96 by PSS	223
Figure 5.5.7	Plan of the test stope showing the seismogenic regions	224
Figure 5.5.8	Plan of test site stope showing seismic activity recorded during four phases of the preconditioning optimisation study	225
Figure 5.5.9	Seismic events of M>1 recorded from the test site between 26/08/96 and 20/10/96 by PSS	226
Figure 5.5.10	Diurnal distribution of seismic data recorded from the test stope W3 panel between 26/08/96 and 20/10/96 by PSS	227
Figure 5.5.11	Schmidt-net (lower hemisphere projection) of poles to all fractures mapped during the optimisation phase	228
Figure 5.5.12	Rose diagrams showing orientation of fractures mapped during the optimisation phase	229
Figure 5.5.13	Gradient and profile lengths measured during the optimisation phase	231
Figure 5.5.14	Ground Penetrating Radar scan, showing ineffective preconditioning when the spacing is greater than 4 m	232
Figure 5.5.15	Ground Penetrating Radar scan, showing the zone of influence of preconditioning holes	233
Figure 5.5.16	Convergence measurements in the test panel during optimisation work	234
Figure 5.5.17	Actual drill times spent per crew to drill 32 production and three preconditioning holes	238
Figure 5.6.1	An example of overhanging hangingwall conditions where the preconditioning hole was drilled at a distance greater than 1 m below the contact between the reef and hangingwall	240

Figure 5.6.2	An example of overhanging hangingwall conditions where the preconditioning hole was drilled at a distance greater than 1 m below the contact between the reef and hangingwall	241
Figure 5.6.3	Examples of improved hangingwall conditions where the preconditioning hole was drilled at about 60 cm below the contact between the reef and hangingwall	242
Figure 5.6.4	Decay of the seismicity with time, following the preconditioning blasts	244
Figure 5.6.5	Cumulative number of events as a function of time	244
Figure 5.6.6	Spatial migrations of the seismic events ahead of the face	245
Figure 5.7.1	Diagrams showing the face-perpendicular preconditioning layout for a three-day cycle	248
Figure 5.7.2	Face-perpendicular preconditioning layout for various mining layouts	249
Figure 5.7.3	Cross-section ahead of the stope face, illustrating the relative positions of the production and preconditioning holes	250
Figure 5.7.4	Hand-held percussion drill machine	251
Figure 5.7.5	Examples of the recommended tie-up configuration of (a) fuse and igniter cord or electric (b) Nonel for integrating the blasting of preconditioning and production holes	253
Figure 6.2.1	The mesh used for the "preconditioning" analyses (after Kullmann *et al.*, 1995)	259
Figure 6.2.2	Maximum principal stress contours in an unaltered discontinuum model (after Kullmann *et al.*, 1995)	260
Figure 6.2.3	Contours of maximum principal stress after applying a pore pressure in the fracture zone immediately ahead of the face (after Kullmann *et al.*, 1995)	261
Figure 6.2.4	Contours of maximum principal stress after applying a pore pressure to the confined rock well ahead of the stope face (after Kullmann *et al.*, 1995)	262
Figure 6.2.5	Comparison of total fracture length derived from a model with actual recorded seismicity subsequent to blasting (after Malan and Spottiswoode, 1997)	268
Figure 6.2.6	Comparison of modelled to actual convergence profiles	269

Figure 6.2.7 Typical time-dependent convergence data measured with an instrument that records in a continuous fashion (after Malan, 1998) 270
Figure 6.2.8 Relationship between continuous (solid line) and daily (dotted line) convergence measurements (after Malan, 1998) 271
Figure 6.2.9 Stress redistribution brought about by preconditioning 274
Figure 7.2.1 Implementation site (Case example 5) 284
Figure 7.2.2 Implementation site (Case example 6) 286
Figure 7.2.3 Implementation site (Case example 8) 287

LIST OF TABLES

Table		Page
Table 1.2.1	Statistics of rock-related accidents and resulting fatalities in South African gold mines from 1990 to 1997 (both incl.)	27
Table 3.4.1	Detail of blast parameters	69
Table 3.4.2	The peak accelerations obtained from the test blasts	75
Table 3.4.3	The detonation velocities measured during the first test blast	78
Table 3.4.4	The detonation velocities measured during the second test blast	78
Table 3.4.5	The detonation velocities measured during the third test blast	79
Table 3.7.1	Mechanical properties of intact rock before and after the test blasts	87
Table 3.9.1	Parameters used for DIGS models	100
Table 4.2.1	Summary of preconditioning blast ratings per panel	123
Table 4.2.2	Occurrence of large (M ≥1.0) seismic events of the preconditioning site	133
Table 4.2.3	Occurrence of large (M ≥1.0) seismic events in association with preconditioning and production activity	134
Table 4.2.4	Average induced daily convergence as a result of production and preconditioning blasting	135
Table 4.2.5	Summary of the various fracture groups	139
Table 5.4.1	Comparison of seismic data recorded by two adjacent PSS networks on WDL South Mine	184
Table 5.4.2	Summary of seismic data recorded before and after the initiation of preconditioning panel 'E' of the test site	186
Table 5.4.3	Summary of characteristics of major fracture types at preconditioning test site (after Grodner, 1997)	196
Table 5.4.4	Summary of the characteristics of the various fracture groups	200
Table 5.4.5	Hole shapes in preconditioned and unpreconditioned panels	208
Table 5.4.6	Safety record for the test site after the start of the preconditioning in May 1995	212
Table 5.4.7	Average cost for timber-supported stopes (stores and labour)	215

Table 5.4.8	Normalised cost to drill and blast one 3.0 m preconditioning hole	216
Table 5.4.9	Total cost of preconditioning for one production blast	216
Table 5.4.10	Comparison of the cost of preconditioning to normal stoping costs	217
Table 5.4.11	Comparison of total costs per m^2 with and without preconditioning	217
Table 5.5.1	Summary of seismic data recorded during preconditioning optimisation study	226
Table 5.5.2	Comparison of face advance rates in preconditioned and unpreconditioned adjacent panels in the test stope	236
Table 5.5.3	Comparison of drilling rates of preconditioning holes	237
Table 5.5.4	Comparison of drilling rates of production holes for adjacent preconditioned and unpreconditioned panels	237

1 INTRODUCTION

South Africa is one of the largest gold producers in the world. The South African gold ore is found in a geological setting called "The Witwatersrand Basin" and consists of extensive, narrow, tabular deposits generally called reefs. Extensive mining has occurred at shallower depths over the last 100 years and today much of the mining occurs at great depth. The mining of reefs at depths in excess of 2000 m induces extremely high stresses on the rockmass in the vicinity of any excavation. In stopes, in particular, such high stresses induced by mining increase the strain energy stored in the rockmass and result in a state of unstable equilibrium. The release of excessive energy in the rockmass can be in the form of the extending of the fracture zone ahead of the stope face and / or the displacement of pre-existing discontinuities either violently or non-violently. The violent release of accumulated strain energy can be described as a seismic event that may result in a rockburst, depending on the magnitude, the distance between the source and the excavation and existing ground conditions around that excavation. If a seismic event results in a rockburst, it can cause extensive damage to underground workings, and varying degrees of injuries and even fatalities.

Although a number of solutions have been suggested by various investigators in the past and some of them have been successfully implemented, the rockburst problem still poses a serious and ongoing hazard to the gold mining industry in South Africa.

1.1 Research problem

The violent release of accumulated strain energy can be in the form of ejection of mining faces into the mine openings at a very high velocity and this phenomenon is called a faceburst.

Data from a rock-related fatal accident database that was compiled by CSIR / Miningtek shows that a total of 216 rock-related fatalities resulted from 134

faceburst incidents throughout the South African gold mining industry during the period 1990 - 1997 (see Table 1.2.1). This figure represents more than 27 percent of the total of 793 rockburst fatalities recorded during this period. The rockburst fatalities are 44 percent of a total of 1808 rock-related fatalities over the same period. The author believes that facebursts comprise a much greater percentage of total rockbursts than this data would lead us to believe because many of the faceburst fatalities were more generally classified as rockburst fatalities. Thus, facebursting is a major concern for the South African gold mining industry. The most problematic reefs are the Ventersdorp Contact Reef (VCR), Carbon Leader (CL) and Composite reefs in which more than two-thirds of all faceburst fatalities occurred.

1.2 Rockburst control research programme

Since 1987, an extensive research project has been carried out by a group of researchers within the Chamber of Mines Research Organisation (COMRO) which, in 1993, became the Division of Mining Technology (known as Miningtek) of the Council for Scientific and Industrial Research (CSIR). The philosophy adopted by researchers working on this project accepts that rockbursts can neither be predicted nor prevented with current knowledge and technology, but may be controlled. Thus, the main objective of the research programme was to develop rockburst control methods to enable mines to operate in areas which are at most risk from seismicity and the resulting rockbursts. In other words, the intention was to control the time and size of seismic events that could result in rockbursts, as well as to minimise the potential damage resulting from such events.

Preconditioning, also called "destress blasting", is a rockburst control technique that involves setting off designed blasting ahead of the stope face. In this way, preconditioning is intended to transfer the stresses further away from the stope face through remobilising the existing fractures in the rockmass.

Table 1.2.1 Statistics of rock-related accidents and resulting fatalities in South African gold mines from 1990 to 1997 (both incl.)

Accident Type	Reef Type	Incidence		Fatality	
		Number	per 10^8 m^2	Number	per 10^8 m^2
Rock-related	Basal	193	7.26	214	8.05
	Carbon Leader	159	20.24	245	31.19
	Composite	15	8.09	20	10.78
	Main	56	10.30	66	12.14
	Vaal Reef	192	8.63	225	10.11
	VCR	297	15.58	374	19.62
	Other reefs*	152	3.88	328	8.37
	Off-reef**	160	-	336	-
	Total / Avg.**	1224	8.70	1808	12.04
Rockburst	Basal	25	0.94	48	1.81
	Carbon Leader	109	13.88	202	25.72
	Composite	12	6.47	17	9.17
	Main	16	2.94	19	3.49
	Vaal Reef	45	2.02	85	3.82
	VCR	157	8.24	242	12.70
	Other reefs*	42	1.07	64	1.63
	Off-reef**	56	-	116	-
	Total / Avg.**	462	3.32	793	5.54
Faceburst	Basal	4	0.15	10	0.38
	Carbon Leader	27	3.44	52	6.62
	Composite	7	3.77	11	5.93
	Main	4	0.74	4	0.74
	Vaal Reef	13	0.58	18	0.81
	VCR	53	2.78	82	4.30
	Other reefs	12	0.31	21	0.54
	Off-reef**	14	-	18	-
	Total / Avg.**	134	0.98	216	1.62

* Other reefs category also contains unspecified reefs.

** Off-reef values are included in total but excluded in average calculations.

Preconditioning techniques have been used in different mining environments around the world since the 1950s and, in many cases, have been found to be very effective in controlling and minimising the effects of rockbursts. The main idea behind these techniques is to detonate a preconditioning blast ahead of a mining face to re-distribute the stress peak further into the solid region ahead of the stope face by eliminating the strain energy "lock-ups" in the asperities of pre-existing or mining-induced fracturing.

In order to quantify the success of preconditioning in highly stressed rock, a better knowledge of the effects of a blast in confined rock is required. An understanding of the genesis and sequence of blast-induced fracturing and the effect of blasting on pre-existing fracturing is crucial for the design of effective preconditioning methods, and for the assessment of the success of preconditioning blasts.

The design of preconditioning blasts involves making a decision on the charge mass, type, hole spacing and diameter, and the position of the charge in the rockmass, as well as the initiation of the charged holes. The quantification of the actual effects of preconditioning on rockmass requires a knowledge of the effect of explosives on rock. Dynamic computer codes can provide insights into the effect of explosives on rock under confined conditions, but very few physical measurements have been made of the effects of explosives under such conditions.

1.3 Objectives of this study

The ultimate objective of this work was to develop and implement preconditioning techniques to control facebursts for the achievement of safer mining in seismically hazardous areas. In order to achieve this main objective, the following goals were also set:

- an investigation of the actual effect of the explosives in the confined and highly stressed rock;
- an understanding of the faceburst and preconditioning mechanisms;

- proving the concept by actual preconditioning experiments at different sites;
- a quantification of the effects of the preconditioning blast on the local rockmass;
- verification of the effects of preconditioning blasts by numerical simulations;
- an optimisation of the preconditioning blasts by varying charge mass, type, hole spacing and diameter, position of the charge in the rock and the initiation sequence of the charges;
- the transfer of the knowledge and experience gained of preconditioning to the mining industry for implementation;
- the development of guidelines for the implementation of preconditioning techniques and determining the requirements for the successful implementation of preconditioning in the industry.

1.4 Outline of the content of the thesis

This thesis consists of 9 chapters. Following this introductory chapter, a summary of an extensive literature review is given in Chapter 2.

The author's initial involvement in the Rockburst Control Research Programme was at the research site established at West Driefontein Gold Mine, where the effects of controlled test blasts were investigated. The findings from these activities are given in Chapter 3. However, this research work had to be stopped after one year, as no funding was made available for continuing the research activities at this site.

The majority of knowledge and experience gained on preconditioning was from the site investigations carried out at the research sites established at Blyvooruitzicht and Mponeng Gold Mines. The results obtained from an extensive monitoring of actual preconditioning blasts in these sites are given in Chapters 4 and 5. While the author had very limited involvement in the investigations on the face-parallel preconditioning discussed in Chapter 4, he headed the research activities involving face-perpendicular preconditioning at Mponeng Gold Mine.